BMC Medical Imaging

RESEARCH

Open Access

Langerhans cell histiocytosis in children: the value of ultrasound in diagnosis and follow-up

Jinjin Yang[1,2†], Xiaohua Huang[1,2†], Zhongtao Bao[1,2†], Jing Xu[1,2], Huimei Huang[1,2], Hongjie Huang[3] and Ling Chen[1,2*]

Abstract

Background Langerhans cell histiocytosis (LCH) is a rare disease, most prevalent in children. Ultrasound is a noninvasive, cheap, and widely available technique. However, systematic elucidation of sonographic features of LCH and treatment related follow-up are relatively few, resulting in overall underestimation of the clinical value of ultrasound in diagnosing and monitoring LCH.

Objective This study aimed to observe the sonographic features of Langerhans Cell Histiocytosis (LCH) comparing with other imaging examinations, and to evaluate the changes of ultrasonography in the follow-up of LCH in children.

Materials and methods Forty-four children (female:male, 19/25; median age, 60 months; range, 8 to 192 months) with LCH were included in this retrospective study. Thirty-one had single-system involvement (SS-LCH), and 13 had multisystem involvement (MS-LCH) among the 44 children. We analyzed the clinical characteristics, ultrasound (US) images, and images from other modalities, including X-ray, computed tomography (CT), and magnetic resonance imaging (MRI). The sonographic characteristics of the various involved organs, particularly bone, thyroid, and liver were analyzed, and the percentage of LCH cases correctly identified by the various imaging modalities were evaluated.

Results Localized worm-like bone defects solid hypoechoic lesions were found in 38 patients with a total of 43 skeletal lesions, which showed solid hypoechoic lesions on US. Five patients showed hypoechoic or hyperechoic areas in the liver. Two patients showed scattered or diffuse irregular hypoechoic areas in the thyroid. Two patients with skeletal and 1 with thyroid involvement showed smaller lesions and lower blood flow after chemotherapy, and 6 lesions involving the liver resolved or were smaller in US review. The percentage of LCH cases correctly identified of US (65.38%) was higher than that of X-ray (21.05%) ($P=0.026$) for skeletal lesions, which was comparable to that of CT and MRI. The overall correctly identified percentage of US for LCH was not significantly different from that of other imaging modalities.

Conclusion LCH can be detected and suspected based on sonographic features. US may be an excellent tool for the diagnosis and follow-up of LCH in children.

† Jinjin Yang, Xiaohua Huang and Zhongtao Bao contributed equally to this work.

*Correspondence:
Ling Chen
chenling0410@fjmu.edu.cn
Full list of author information is available at the end of the article

Highlights

- Pediatric Langerhans cell histiocytosis (LCH) can be detected and suspected based on sonographic features.
- Ultrasound examination outperforms other imaging modalities in the initial evaluation of pediatric LCH.
- Ultrasound may be an ideal imaging tool for post-treatment follow-up of LCH in children.

Keywords Ultrasound, Langerhans cell histiocytosis, Children

Background

Langerhans cell histiocytosis (LCH) is a rare disease characterized by the accumulation of cells thought to be derived from $CD1\alpha^+$ or $CD207^+$ dendritic cells (DCs) or macrophagesb in various tissues [1]. LCH affects individuals of all ages, and the peak incidence is between 1 and 4 years of age [2, 3]. LCH can affect any organ or site. The clinical manifestation and course of LCH are remarkably variable, ranging from a self-healing single-system disease to a widely disseminated multisystem disease [4]. The skeletal system is most affected in children with LCH, known as eosinophilic granuloma of bone (EGB), which accounts for approximately 75% to 80% of LCH cases [5], followed by the skin, pituitary, liver, spleen, lungs, and lymph nodes [6, 7]. Additionally, the liver, spleen, and bone marrow are risk organs (ROs) for patients with LCH, whereas thyroid involvement is relatively rare.

Currently, patients with single-system involvement (SS-LCH) are typically treated with surgery, which is associated with favorable outcomes. However, patients with multisystem involvement (MS-LCH), particularly those with RO involvement, usually require multimodality treatment and have variable prognoses [6]. During clinical diagnosis and treatment, single-focal SS-LCH is a self-limiting disease [8]. If appropriate treatment is provided, the prognosis is usually good [8]; MS-LCH depends on which organs are involved, but whether ROs are involved is directly related to its efficacy and prognosis [6]. A systematic and proactive treatment plan is needed for MS-LCH patients with RO involvement [6]. In addition, the 5-year recurrence rate of SS-LCH is less than 20%, while that of MS-LCH is 50% or less. Recurrence usually involves the same organ system but may also involve different parts [6] and may develop from SS-LCH to MS-LCH [9]. As such, an early and accurate diagnosis of LCH is crucial to improve the survival of LCH patients.

Clinically, the diagnosis of LCH is made by immunohistochemical pathological dendritic cell-specific markers $CD1\alpha^+$ or $CD207^+$. However, due to its nonspecific clinical manifestations, pretreatment imaging examinations, such as ultrasound (US), X-ray, computed tomography (CT), and magnetic resonance imaging (MRI), are necessary. To date, many ongoing studies have focused on LCH; unfortunately, most of these studies were reported as case reports [8, 10–12]. Moreover, systematic elucidation of the sonographic features of LCH and treatment-related follow-up are relatively few, resulting in an overall underestimation of the clinical value of US in diagnosing and monitoring LCH. Therefore, this study aimed to analyze the relevant US features in LCH, to compare US with other imaging examinations and to summarize the changes in US characteristics in the treatment of LCH.

Methods

Subjects

This retrospective study was approved by the local institutional review board, and the requirements for informed consent forms were waived by Branch for Medical Research and Clinical Technology Application Ethics Committee of the First Affiliated Hospital of Fujian Medical university. The diagnosis of LCH was based on clinical, radiological, and histological findings. The confirmation of diagnosis of LCH was made by pathological analysis with dendritic cell-specific markers $CD1\alpha^+$ or $CD207^+$. We defined the involved organs base on surgical or biopsy pathology. For additional organ or tissue involvement, diagnoses were made by clinicians who assessed clinical examinations, symptoms, relevant laboratory findings, imaging, and lesion resolution or reduction after treatment for LCH. We retrospectively reviewed the clinical data, US images, and other imaging (X-ray, CT, and MRI) data of pediatric patients (under 18 years old) with suspected LCH in our hospital from January 2013 to March 2023. Finally, forty-four children (female:male, 19/25) were enrolled in the study, ranging in age from 8 to 192 months. Patients were selected according to the following criteria: (i) pathologically proven LCH by surgery or biopsy; and (ii) at least one of the following imaging examinations was performed: US, X-ray, CT, and MR; and (iii) all patients undergo a skeletal survey through a physical examination by clinical doctors. Patients were excluded according to the following conditions: (i) the presence of rheumatic immune disease or other genetic or metabolic diseases; (ii) the absence of imaging data for the first visit to our hospital; and (iii) poor imaging quality. Finally, three cases were ruled out.

The protocol for whole body evaluation of LCH in children was followed the European guidelines [4].

US examination

In the study, a variety of commercially available US instruments with high-frequency line array probes for 5–18 MHz and low-frequency convex array probes for 1–5 MHz were used, including IU22 (Philips, Amsterdam, Netherlands), EPIQ 5 (Koninklijke Philips N.V., Amsterdam, Netherlands), and ACUSON Sequoia (Siemens, Washington, USA). Children who could not cooperate were sedated with oral 10% chloral hydrate 0.3–0.5 ml/kg body mass.

Other imaging examinations

Other imaging examinations were obtained with the machines and parameters described below.

X-ray: GE Definium 6000 DR and SIEMENS YSIO Max medical diagnostic X-ray machines with the following parameter settings: current, 30 mA; voltage control, 65 kV; and scan time, 0.25 ms.

CT: Toshiba Aquilion 16-row spiral CT with the following scanning parameters: tube voltage, 120 kV; tube current, 350 mA; and scanning layer thickness, 1 mm. Toshiba Aquilion one 320-row CT machine with the following scanning parameters: tube voltage, 120 kV; tube current, 300 mA; and layer thickness, 0.5 mm.

MR: 1.5 T Toshiba EXCELART Vantage MRT-1503 Atlas-X and 3.0 T Siemens MAGNETOM Verio MR scanners with a 20-channel combined head and neck coil or 8-channel body phased array coil. Conventional MRI sequences included T1WI, T2WI, DWI and contrast enhanced fs-T1WI. T1WI: TR, 250–690 ms; TE, 2.5–24 ms: T2WI: TR, 2200–6000 ms; TE 57–120 ms; contrast enhanced fs-T1WI: TR, 500–740 ms; TE, 9.9–24 ms. The contrast agent was Gd-BOPTA at a dose of 0.1 mmol/kg.

Imaging analysis

US examination was particularly focused on the abdomen, neck, skin, and skeletal system. Ultrasonographic observations included (i) abnormalities in the morphology, size, and echogenicity of organ tissues and focal lesions; (ii) the location, number, size, echogenicity, borders, and color Doppler flow image (CDFI) characteristics of focal lesions; (iii) the sonographic characteristics of tissues surrounding focal lesions, such as bone, bile ducts, and portal veins; (iv) abnormalities in the lymph nodes near the affected organs or tissues; and (v) the accumulation of fluid in the abdominal cavity. In addition, in describing the sonographic changes in the thyroid gland, we defined the image of multiple adjacent hypoechoic areas in the parenchyma separated by linear hyperechoic bands forming pseudo nodules as giraffe like-skin changes.

Other imaging examinations were performed on different systems throughout the whole body, focusing on the following: (i) which organ was involved in the suspected LCH; (ii) the location, size, density, and signal intensity of the LCH lesion; and (iii) the evaluation of the surrounding lesion and bone destruction.

Follow-up observation

The follow-up period was 1–72 months. The ultrasonographic follow-up observations included (i) changes in the shape, size, echogenicity, and blood flow signal of the involved organs and tissues in LCH after surgery or drug treatment and (ii) the observation of new lesions in other areas.

Statistical analysis

Statistical analysis was performed using SPSS 26.0 software. The statistical information is presented as the median (interquartile range [IQR]). The different imaging modality findings were compared with histopathological results.The diagnostic accuracy rate = the number of correctly diagnosed LCH lesions/the number of lesions for which a certain examination was performed. The chi-square test Bonferroni's multiple comparisons method was used to compare the diagnostic accuracy of different imaging modalities in the SS-LCH and MS-LCH groups. A P value < 0.05 indicated that the difference was statistically significant. Bar charts were made using Microsoft Excel 2023 software.

Results

Baseline clinical characteristics

The cohort consisted of 44 children with LCH, including 31 SS-LCH (19 male and 12 female) and 13 MS-LCH (6 male and 7 female) patients. The median (IQR) ages of SS-LCH and MS-LCH patients were 34.5 (28–108) and 36 (16–156) months, with ranges of 8 months to 168 months and 8 months to 192 months, respectively. Of the 31 patients with SS-LCH, the lesions of 25 skeleton involved had surgical pathology, and the remaining 4 patients had biopsy pathology. Among the 13 patients with MS-LCH, 11 patients had skeleton surgical pathology, and 2 liver and 1 skin had biopsy tissue sampled. For additional organ or tissue involvement, diagnoses were made by clinicians. The main clinical manifestations included a local palpable mass (SS-LCH/MS-LCH: 21/8), local pain (4/4), abnormal movement (2/1), epigastric discomfort (0/5), palpable thyroid enlargement (0/2), rash (2/3) and asymptomatic (2/0). 8 patients had blood abnormal liver function (SS-LCH/MS-LCH: 3/5), and 2 had blood thyroid function abnormal with MS-LCH. Of

the 31 patients with SS-LCH, the lesions of 25 were surgically removed, and 6 patients were treated medically. Among the 13 patients with MS-LCH, 4 were treated surgically, 2 were treated with medical drugs, and 7 were treated with medical drugs after surgical removal of lesions involving bone. Twenty patients whose initial symptoms were body masses preferred to choose or were advised by doctors to have an Ultrasonic scanning as first imaging exam, 7 were for X-ray, 2 were for CT, and none for MRI. The sites of LCH involvement in the children in this study are shown in Fig. 1. There were 3 SS-LCH children with skin involved opted out of further radiographic evaluation after clinicians found no skeletal abnormalities on physical examination during the initial visit, and the all remaining children had at least one skeletal imaging examination. No patients underwent contrast-enhanced CT, all patients had non contrast CT (NCCT). There were 15 patients (SS-LCH: MS-LCH, 10/5) underwent a MRI enhanced examination for skeletal lesions.

Sonographic features

Skeletal US sonography

A total of 30 skeletal lesions detected by US were came from 26 children with clinical manifestations including localized palpable masses, localized pain, and motor abnormalities. Specifically, bone destruction was found in 24 lesions, which showed local osteolytic and worm-like bone destruction with irregular margins in the bone defects. Twenty-two lesions were solid hypoechoic lesions with clear borders within the area of bone loss. Eighteen lesions showed internal homogeneous echogenicity, 4 lesions had varying degrees of necrosis, and 22 lesions demonstrated varying degrees of internal blood flow signals (Figs. 2a-d, 3a-d and 4a-g).

Abdominal US sonography

In the patients with SS-LCH, the liver was mildly enlarged in 3 patients, and the echogenicity of the liver parenchyma was rough and inhomogeneous. Two children with skin involvement showed no abnormalities on abdominal sonograms. In the patients with MS-LCH, the sonogram showed that (i) the liver was enlarged to varying degrees in 5 patients, in whom hypoechoic or hyperechoic areas were seen in the liver, with either scattered or diffuse distribution, and the hypoechoic areas were distributed along the intrahepatic bile ducts in 2 patients, which was accompanied by a thickening of the portal vein wall and gallbladder wall. (ii) The common bile duct wall and intrahepatic bile duct wall were thickened and their echogenicity was increased in 2 patients, with localized narrowing or dilatation of the intrahepatic bile duct. (iii) Mild splenomegaly was found in 2 patients, with scattered hypoechoic areas found in the parenchyma. (iv) Two patients showed lymph node enlargement in the

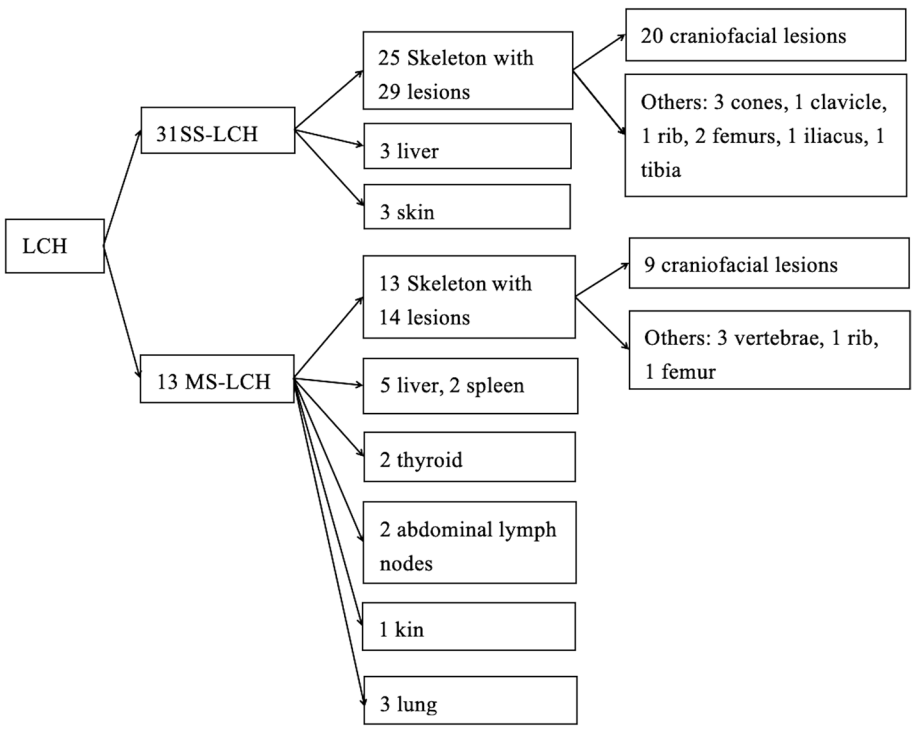

Fig. 1 Distribution of LCH involvement in children

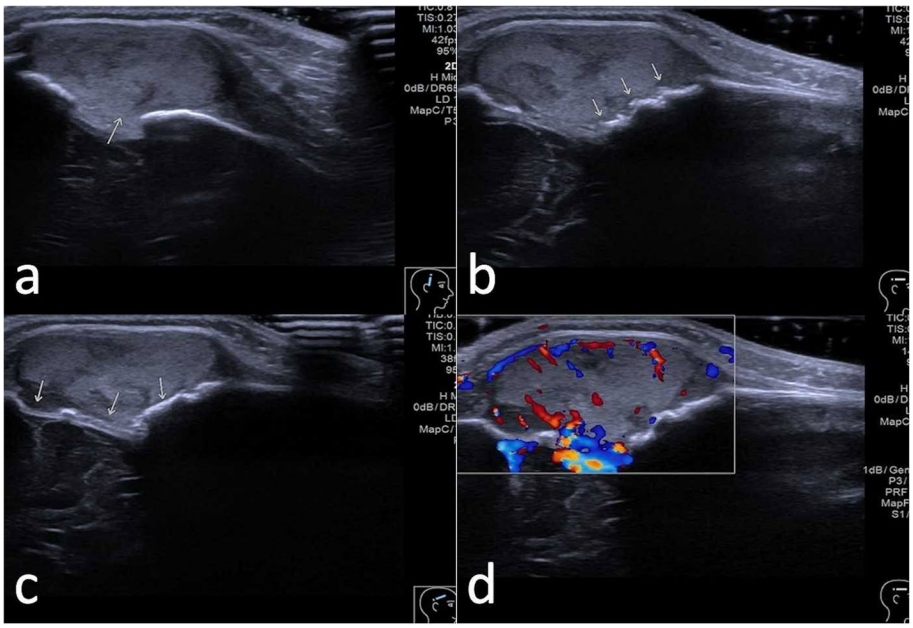

Fig. 2 Imaging of a child with SS-LCH who had multiple lesions in the right temporal region. **a-c** Bone defect area with irregular margins and internal solid hypoechogenicity. **d** CDFI examination showed a rich blood flow signal within the lesion

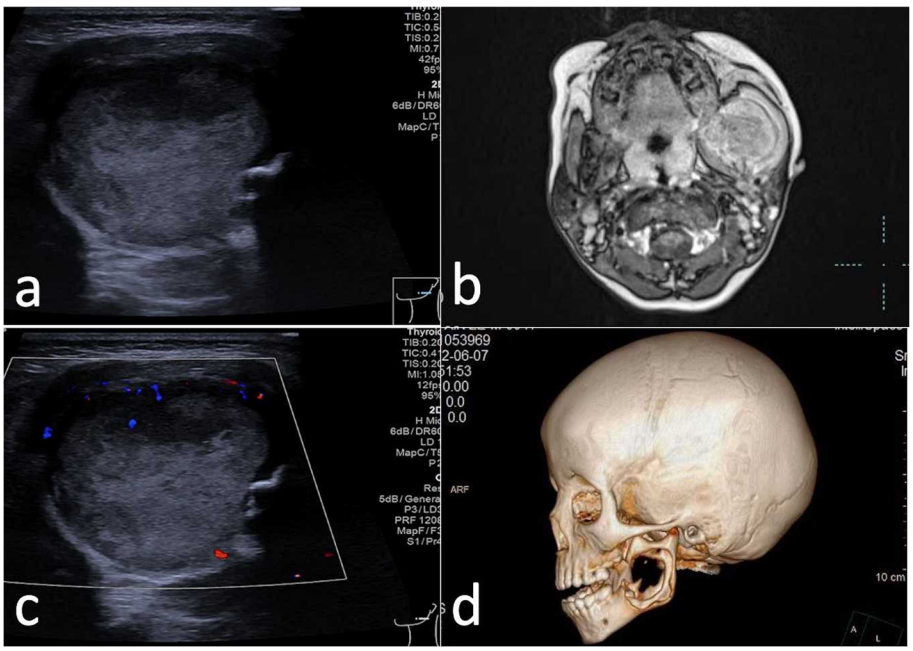

Fig. 3 Imaging in a child with SS-LCH who had a single lesion in the left mandible. **a** Bone defect area with irregular margins and internal solid hypoechogenicity. **b** CDFI examination showed a few short streaks of blood flow signal within the lesion. **c** MR T1W1 enhanced scan showing a mass in the left mandible with significant enhancement and peripheral bone destruction. **d** Three-dimensional CT reconstruction imaging showing osteolytic destruction of the mandibular angle to the ascending mandibular branch

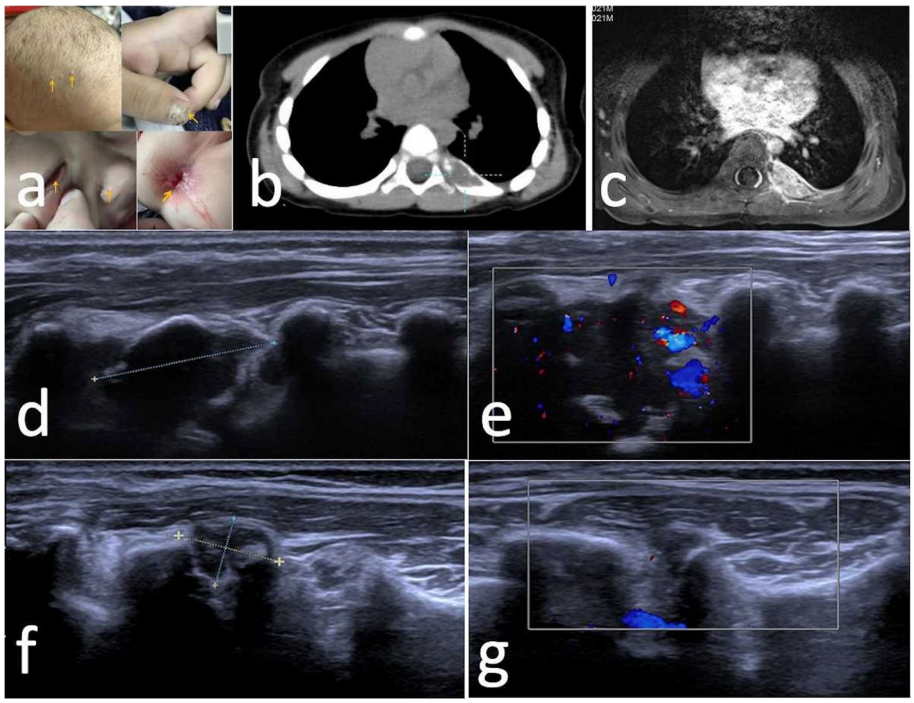

Fig.4 Imaging in a child with MS-LCH. **a** Physical signs of scalp, nails, eyelids, and anus. **b** CT shows bone destruction with soft tissue density shadows inside and its CT value was 34Hu. **c** MR T1W1 enhanced scan showing a mass in the left seventh posterior rib, with significant enhancement and poorly displayed local rib bone. **d**-**e** Sonogram showing a left posterior seventh rib lesion with rich blood flow signal. **f**-**g** A review four months after first-line chemotherapy showed a markedly reduced lesion and blood flow signal on the sonogram

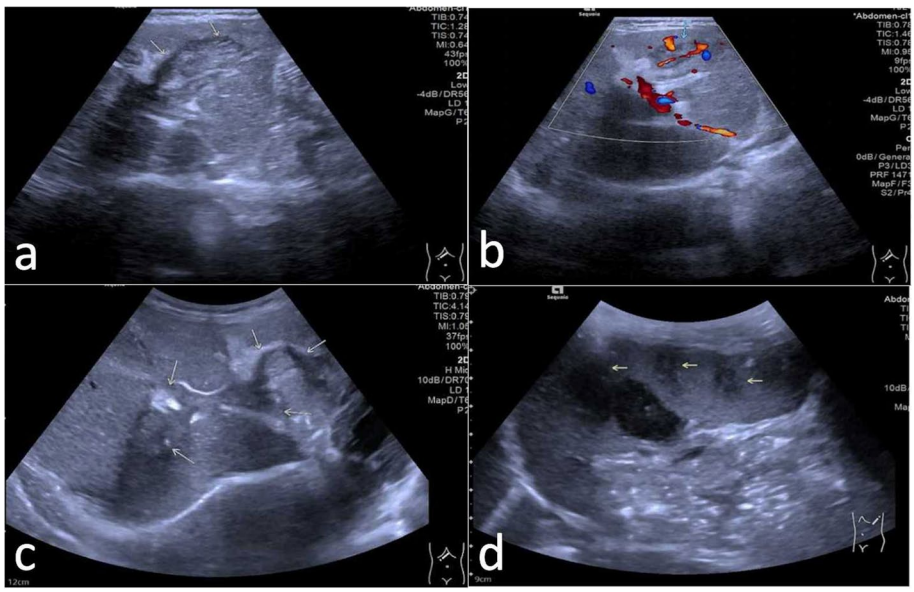

Fig. 5 Imaging in a child with MS-LCH. **a**-**c** Intrahepatic portal vein wall thickening and scattered hypoechoic areas along the bile ducts. **d** Splenomegaly with scattered hypoechoic areas seen in the spleen

hepatic hilar region, and 1 patient showed a small amount of fluid in the abdominal cavity (Figs. 5a-d and 6a-c).

Neck and skin US sonography

Two patients with MS-LCH showed abnormal thyroid morphology, with scattered or diffuse irregular hypoechoic areas within the gland. One patient had multiple adjacent hypoechoic areas, forming changes similar to giraffe-like skin; CDFI examination showed a slightly enriched blood flow signal in the hypoechoic area. US showed no obvious abnormalities in the cervical lymph nodes (Fig. 7a-b).

Three patients with SS-LCH showed single or multiple hypoechoic nodules in the subcutaneous fat layer with

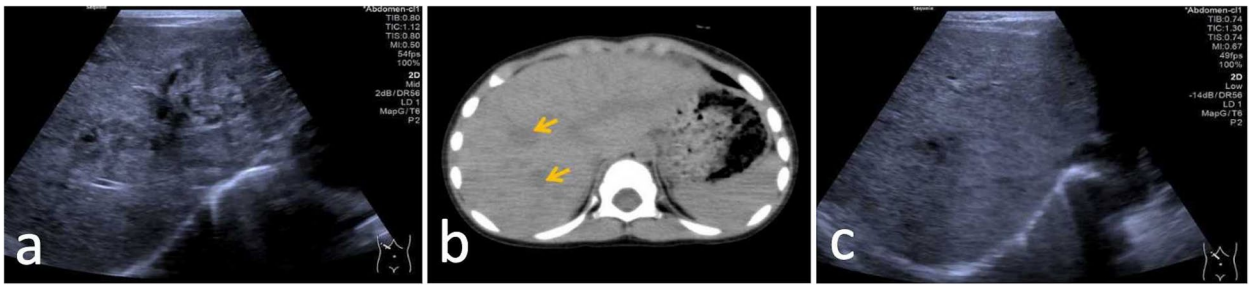

Fig. 6 The same patient as in Fig. 4. **a** The liver parenchyma was rough and inhomogeneous, accompanied by thickening of the portal vein wall and dilated intrahepatic bile ducts. **b** CT scan showing dilated intrahepatic bile ducts and their surrounding hypodense foci. **c** US showed a significant reduction of the intrahepatic lesions four months after first-line chemotherapy

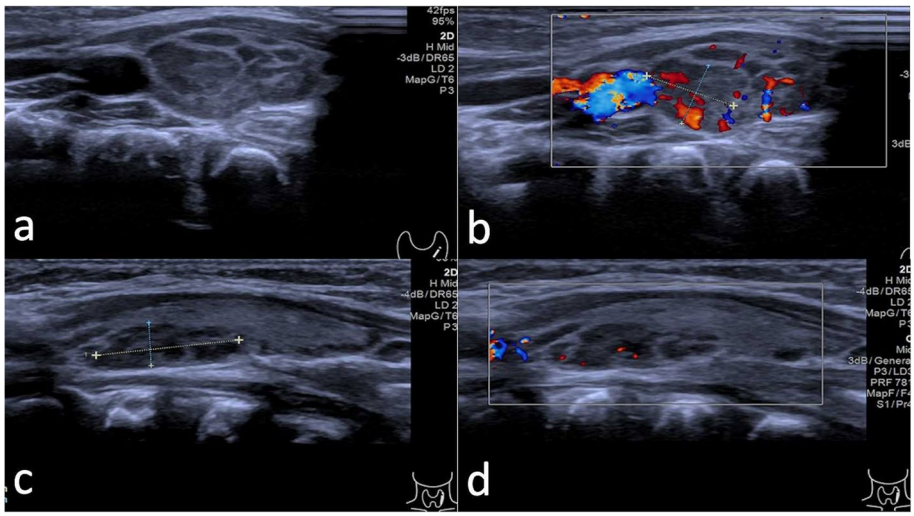

Fig. 7 The same patient as in Fig. 4. **a** Multiple hypoechoic nodules in the left lobe of the thyroid gland, forming changes similar to giraffe-like skin. **b** Rich blood flow signals can be seen in hypoechoic nodules. **c-d** After four months of first-line chemotherapy, the lesion significantly shrank, and the blood flow signal decreased on follow-up examination

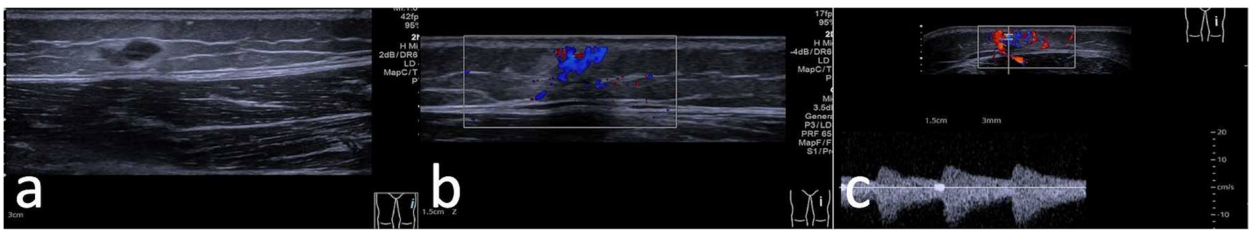

Fig. 8 Imaging in a child with SS-LCH. **a-b** Four hypoechoic nodules of varying sizes in the subcutaneous layer of the left middle thigh (**a**), and abundant blood flow signals in the nodules on CDFI examination (**b**). **c** pulsed wave Doppler (PW) examination indicated low resistance arterial type spectrum

unclear boundaries, uneven internal echoes, and abundant blood flow signals at the edge of the nodules on CDFI examination (Fig. 8a-c).

US sonography in the follow-up

For the patients with posttreatment follow-up, 1 SS-LCH and 2 MS-LCH patients showed smaller EGB lesions and reduced blood flow signals after chemotherapy (Fig. 4d-f). The echogenicity of 3 patients with SS-LCH liver involvement became normal after six months of treatment. Among the patients with MS-LCH, 3 patients had smaller lesions in the liver in posttreatment follow-up (Fig. 6c). One patient with thyroid involvement underwent a posttreatment US examination, which showed that the intraglandular lesion had decreased in size and that the blood flow signal was reduced (Fig. 7c-d). In 28 of 29 patients who underwent surgical removal of lesions, no lesion recurrence or new lesions were found; in the remaining patient, who had MS-LCH, a new lesion above the upper mediastinal thymus gland appeared after 17 months of follow-up.

Comparative analysis with other imaging

In terms of the skeletal system, 18, 12, 16, and 15 SS-LCH patients underwent US, X-ray, NCCT, and MR examinations, with accuracies of 61.11% (11/18), 25.0% (3/12), 31.25% (5/16), and 86.67% (13/15) for EGB, respectively. Among MS-LCH patients, 8, 7, 10, and 13 patients underwent US, X-ray, NCCT and MR examinations, with accuracies of 75.0% (6/8), 14.28% (1/7), 50.0% (5/10), and 84.61% (11/13) for EGB, respectively. The diagnosis of skeletal lesions by US, X-ray, NCCT, and MR examinations, including the number of correct diagnoses of EGB, misdiagnoses, missed diagnoses and undetected diagnoses, are shown in bar charts (Figs. 9 and 10, Tables 1 and 2).

For diagnosing nonskeletal lesions, all 3 children with SS-LCH with liver involvement underwent abdominal US and MR examination, and 2 underwent NCCT. However, liver abnormalities were detected only by US examination; no abnormalities were found on NCCT or MR. Three children in the SS-LCH group had US

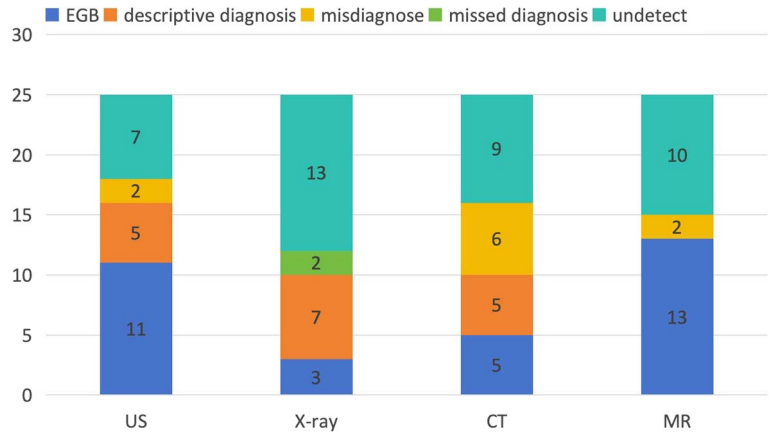

Fig. 9 Different imaging findings of the skeletal system involved in SS-LCH

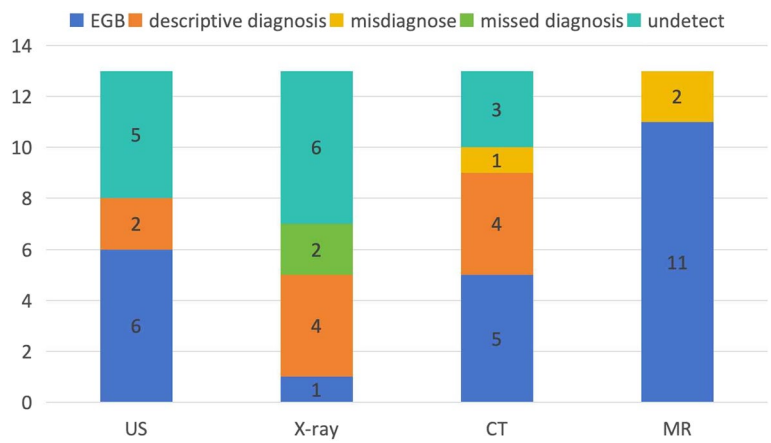

Fig. 10 Different imaging findings of the skeletal system involved in MS-LCH

Table 1 Comparison of the diagnostic accuracy rate of US and other imaging for the diagnosis of skeletal EGB in LCH (n/N, %)

	SS-LCH	MS-LCH	Total
US	11/18 (61.11)[a,b]	6/8(75.00)[a,b]	17/26(65.38)[a]
X-ray	3/12(25.00)[b]	1/7(14.28)[b]	4/19(21.05)[b]
CT	5/16(31.25)[b]	5/10(50.00)[a,b]	10/26(38.46)[a,b]
MR	13/15(86.7)[a]	11/13(84.61)[a]	24/28(85.71)[a,b]
χ2	14.092	10.587	9.252
P	0.003	0.014	0.026

In the same column, for those labelled with different letters, there was a statistical difference in the comparison of the two methods; for those labelled with the same letter, there was no statistical difference in the comparison of the two methods

Abbreviations: *EGB* eosinophilic granuloma of bone

Table 2 Comparison of overall diagnostic accuracy of US with other imaging modalities in the diagnosis of LCH (n/N, %)

	SS-LCH	MS-LCH	Total
US	12/24(50.00)[a,b]	7/9(77.78)[a,b]	19/33(57.58)[a,b]
X-ray	3/12(25.00)[b]	1/7(14.28)[b]	4/19(21.05)[b]
CT	5/18(27.78)[b]	5/10(50.00)[a,b]	10/28(35.71)[b]
MR	13/18(72.22)[a]	11/13(84.61)[a]	24/31(77.42)[a]
χ2	11.598	11.094	18.667
P	0.09	0.01	0.000

In the same column, for those labelled with different letters, there was a statistical difference in the comparison of the two methods; for those labelled with the same letter, there was no statistical difference in the comparison of the two methods

examinations of palpable skin masses, which were misdiagnosed as nodular fasciitis and hemangioma, but no other imaging examinations were performed. Among the MS-LCH patients, 5 children had liver involvement. These 5 children underwent US examinations, 3 also underwent NCCT, and 2 also underwent MRI examinations. They were all diagnosed with LCH by US, and the position and size changes in the liver shown in either NCCT or MRI were generally consistent with the US findings. US indicated thyroid involvement in 2 children, while no significant abnormalities were seen on NCCT or MRI examinations.

As shown in Table 1, the percentage for the diagnosis of skeletal EGB in LCH cases correctly identified of US (65.38%) was higher than that of X-ray (21.05%) ($P=0.026$), which was comparable to that of NCCT and MRI examinations for skeletal lesions. As shown in Table 2, The overall correctly identified percentage of US for LCH was not significantly different from that of other imaging modalities (X-ray, CT, and MRI) by chi-square test Bonferroni's multiple comparisons method ($P>0.05$).

Discussion

This study aimed to observe the sonographic features of LCH comparing with other imaging examinations, and to evaulate the changes of ultrasonography in the treatment of LCH in children. A total of 44 patients were included in the study. This study showed that sonographic features of the various involved organs, particularly bone, thyroid, and liver were characteristic in pretreatment and posttreatment. For skeletal lesions, the diagnostic accuracy rate of US was higher than that of X-ray, which was comparable to that of CT and MRI examinations. The overall diagnostic accuracy rate of US for LCH was not significantly different from that of other imaging modalities.

US evaluation for LCH

LCH can affect any organ or site, but the skeletal system is predominantly involved. Moreover, unifocal rather than multifocal lesions are more common. Therefore, X-rays and CT are usually preferred imaging modalities in evaluating LCH in clinics. However, US has rarely been used in the past to confirm bone involvement in EGB [13]. With the evolution and development of musculoskeletal US, US has been shown to be feasible and is increasingly used to diagnose skeletal diseases. The benefits of US in skeletal disease diagnosis are due to the use of increasingly high-frequency probes, providing a strong ability (almost comparable to that of MRI) to visualize soft-tissue lesions in the body and allowing fine discrimination of the muscles and superficial tissue nerve structures [14]. In the current study, we found that for children with EGB whose initial symptoms were body masses, especially those occurring in the craniofacial region, US was the most suggested examination. The sonogram features in these patients included localized bone destruction and hypoechoic solid masses with blood flow signals within the bone loss area, which were consistent with previous studies [15]. As the disease progresses, fibrosis, focal bleeding, and necrosis occur within the lesion. In this study, one case of EGB was misdiagnosed as hematoma due to the presence of many liquefied areas. Moreover, one patient with a temporal mass showed obvious swelling and pain at the initial visit. The lesion was misdiagnosed as an inflammatory mass since the patient showed an increased white blood cell count. After anti-inflammatory treatment, the symptoms of this patient and the follow-up US showed no significant changes. Finally, the biopsy sample analysis confirmed that the lesion was an LCH lesion.

LCH rarely affects the liver, and most patients with liver lesions have MS-LCH. Patients with liver involvement are considered high-risk patients. A study [16] found that the 1-year survival rate of high-risk LCH patients is only 33%, the 5-year survival rate is 25%, and the survival

rate of MS-LCH without high RO involvement is 98.4% [17]. Therefore, early diagnosis is very important. LCH is histologically divided into four different stages: initial proliferation, intermediate granuloma, xanthoma, and late fibrous stages [18]. In this study, US examination of SS-LCH patients showed a coarse, inhomogeneous liver parenchyma, possibly due to the initial proliferation stage of the lesion. For MS-LCH patients, US showed scattered or diffusely distributed hypoechoic areas in the liver, some of which were distributed along the bile duct or portal vein, accompanied by a thickening of the wall of the portal vein and the wall of the biliary system. This may be due to the robust infiltration of inflammatory cells at the granulomatous stage, confirming that LCH was an inflammatory reactive disease initially. As the disease progresses into the xanthoma stage, lipid deposits accumulate in the liver, presenting as hyperechoic areas on US and low density areas on NCCT (as shown in Fig. 6). In addition, in this study, there were 2 patients who showed involvement of the spleen and lymph nodes, which are rich in the reticuloendothelial tissue and susceptible to LCH. Therefore, attention should be given to observing abnormalities in the spleen and lymph nodes during abdominal US examination.

Skin lesions are the second most common clinical manifestation of LCH, accounting for approximately 30–60% of cases [19], particularly in infants. SS-LCH skin lesions are observed in 2% of the total LCH population [6]. LCH lesions have different forms and severities, with crusts or squamous papules and papules in the dermis as the most common manifestations. Rare lesions include angiomatous lesions, chickenpox-like rashes, or purpura [6]. In this study, one child initially presented with scalp, nail, eyelid, and anus involvement and received routine treatment for a period in the dermatology department, but no obvious improvement was found. Histopathological analysis of a tissue biopsy was then performed, which confirmed a diagnosis of LCH. Subsequently, lesions were found in his rib (as shown in Fig. 4). Ultrasonography is preferred when the clinical manifestation of subcutaneous tissue lesions is a palpable mass on the body surface. In this study, hypoechoic nodules were found in 2 lesions in the subcutaneous fat layer of patients with SS-LCH; these lesions were misdiagnosed as other neoplastic lesions because of the rare skin involvement in SS-LCH and the nonspecific US manifestations. In this regard, color Doppler US could assess the blood supply of the nodules and ensure the safety of surgery.

LCH involving the thyroid gland is rare in MS-LCH and mostly occurs in a subset of adults with MS-LCH [20–22]. Patten et al. [20] summarized the cases of 66 patients with thyroid gland involvement (both adults and children) and found that 59% of patients presented with diffuse lesions, 25.8% presented with nodular enlargement, and 19.7% presented with hypothyroidism. In the present study, two patients with thyroid involvement showed diffuse hypoechoic areas in the unilateral lobes, forming a "giraffe-like" appearance on the sonogram. The diagnosis was made in combination with abnormal blood thyroid function tests, other systemic manifestations, and the hypoechoic areas decreased after treatment, further confirming the US diagnosis. The prognosis of thyroid LCH is usually good, but a long follow-up is necessary, as multiple systems may be involved.

Other imaging examinations for LCH

Of note, the clinical presentation of LCH is complicated and varied, and its diagnosis ultimately depends on histopathology; the main role of diagnostic imaging is to screen for suspected LCH, assess the extent of the disease, confirm multisystem involvement, and monitor the treatment response [4].

For skeletal lesion detection, this study showed that X-ray examination can preliminarily detect the location of skeletal lesions and assess the degree of bone destruction; however, X-ray examination still suffered from the limitations of low-density resolution, poor display of the internal structure of EGB lesions. This study found that US can provide excellent diagnostic confidence in the diagnosis of LCH, especially for children with EGB. In this study, the comparison of X-ray and US showed that US more clearly displayed the periosteal soft tissue changes, but it could not display bone destruction as well as X-ray. CT is a cross-sectional scan approach that can detect lesions that are poorly displayed or missed on X-ray with a better demonstration of the internal structure of the lesion. However, it had been found that the accumulation of CT doses increases the competitiveness of cells with cancerous potential, and that there was a positive correlation with the risk of hematologic malignancies [23, 24]. Ultrasonography cannot replace CT in assessing localized LCH, but it can reduce the number of follow-up CT examinations [15]. Thus, it is importance of minimizing radiation exposure, particularly in pediatric populations, and need for judicious use of imaging modalities in clinical practice. MRI was inferior to X-ray and CT for showing the morphology of skeletal lesions, while it showed better soft tissue resolution and allowed multiaxis multisequence scanning, which is of high value in determining the nature of the lesion. Furthermore, MRI has high diagnostic accuracy. Nevertheless, the biggest challenge of MRI examination in children with LCH was that children find it difficult to tolerate the MRI acquisition procedure, resulting in severe motion artifacts in addition to its expensive price. Compared to CT and MRI, US is highly flexible, allowing various

cross-sectional views during examination, with the most representative views selected for analysis and diagnosis. Although the presentation of focal LCH lesions in children's bones is not specific with US, the features are sufficient to suggest a preliminary diagnosis and to monitor the evolution of the lesion during treatment [15]. For non-skeletal lesion detection, three children with SS-LCH and liver involvement underwent both abdominal US and MRI, and two also had NCCT. However, liver abnormalities were detected only by ultrasound, with no abnormalities found on NCCT or MRI. Similarly, in MS-LCH patients, ultrasound indicated thyroid involvement in two children, while NCCT and MRI showed no significant findings. This discrepancy may be attributed to the lack of contrast-enhanced CT or MRI of the abdomen or neck in our cohort. Ultrasound's interactive nature allows real-time observation and history-taking, potentially enhancing diagnostic yield in such cases.

In this study, US, X-ray, NCCT, and MRI were used to evaluate local lesions. However, it should be noted that the staging and classification of LCH depend on whole-body imaging scans [25], and whole-body imaging is not available with US. In this regard, the whole-body assessment of LCH still depends on other imaging examinations.

Our study has several limitations. First, as our hospital is not a hospital specializing in the care of children, the relatively small sample size limits further identification of the clinical and imaging features of LCH. Second, since this was a retrospective study, the imaging examination methods and machines were not the same for all patients, and the time intervals for follow-up observation were not consistent for all patients. Third, our follow-up of these patients was relatively short, which hindered our further investigation of treatment-related imaging alterations.

Conclusions

The diagnosis of LCH is extremely challenging, and the various imaging examinations are mutually complementary. This study shows that LCH can be detected and suspected based on sonographic features, which can provide clinicians with direct visualization information. Compared to other imaging modalities, ultrasound is non-radioactive, cost-effective, and convenient. It also does not require contrast agents to assess lesion vascularity, making it a useful tool for guiding biopsies or surgery at the bedside. Additionally, it may be an ideal imaging tool for evaluating treatment-related changes in LCH. Clinicians ought to have a thorough understanding of the optimal imaging techniques suitable for various organs and systems, which is essential for the timely diagnosis of conditions.

Authors' contributions

Ling Chen, Zhongtao Bao conceived the idea for the work. Jinjin Yang wrote the manuscript. Ling Chen, Zhongtao Bao, Jing Xu and Hongjie Huang prepared and interpreted figures. Jinjin Yang, Xiaohua Huang, Huimei Huang analyzed and add interpreted the data. Ling Chen, Zhongtao Bao reviewed the manuscript. All authors have approved the submitted version.

Funding

The study was supported by the Startup Fund for Scientific Research of Fujian Medical University (Grant number: 2019QH1111) and Fujian Provincial Finance Project (Grant number: BPB-2023CL). The funding bodies played no role in the design of the study and collection, analysis, and interpretation of data and in writing the manuscript.

Data availability

The datasets used during the current study are available from the corresponding author on reasonable request.

Declarations

Ethics approval and consent to participate

The studies involving human participants were reviewed and approved by Branch for Medical Research and Clinical Technology Application Ethics Committee of the First Affiliated Hospital of Fujian Medical university. Authors confirm that all methods were in accordance with the relevant guidelines and regulations. The requirements for informed consent forms were waived.

Consent for publication

Not applicable.

Competing interests

The authors declare no competing interests.

Author details

[1]Department of Ultrasound Medicine, First Affiliated Hospital, Fujian Medical University, Fuzhou 350005, China. [2]Department of Ultrasound Medicine, National Regional Medical Center, Binhai Compus of First Affiliated Hospital of Fujian Medical University, Fuzhou 350212, China. [3]Department of Radiology, First Affiliated Hospital, Fujian Medical University, Fuzhou 350005, China.

Received: 20 August 2023 Accepted: 20 January 2025
Published online: 29 January 2025

References

1. Emile JF, Abla O, Fraitag S, Horne A, Haroche J, Donadieu J, et al. Revised classification of histiocytoses and neoplasms of the macrophage-dendritic cell lineages. Blood. 2016;127(22):2672–81.
2. Horibe K, Saito AM, Takimoto T, Tsuchida M, Manabe A, Shima M, et al. Incidence and survival rates of hematological malignancies in Japanese children and adolescents (2006–2010): based on registry data from the Japanese Society of Pediatric Hematology. Int J Hematol. 2013;98(1):74–88.
3. Zinn DJ, Chakraborty R, Allen CE. Langerhans cell histiocytosis: emerging insights and clinical implications. Oncology (Williston Park). 2016;30(2):122–32, 139.
4. Haupt R, Minkov M, Astigarraga I, Schafer E, Nanduri V, Jubran R, et al. Langerhans cell histiocytosis (LCH): guidelines for diagnosis, clinical work-up, and treatment for patients till the age of 18 years. Pediatr Blood Cancer. 2013;60(2):175–84.
5. Buckley L, Nuttall T. Feline eosinophilic granuloma complex(ities): some clinical clarification. J Feline Med Surg. 2012;14(7):471–81.
6. Krooks J, Minkov M, Weatherall AG. Langerhans cell histiocytosis in children: History, classification, pathobiology, clinical manifestations, and prognosis. J Am Acad Dermatol. 2018;78(6):1035–44.
7. Cui L, Wang CJ, Lian HY, Zhang L, Ma HH, Wang D, et al. Clinical outcomes and prognostic risk factors of Langerhans cell histiocytosis in children: Results from the BCH-LCH 2014 protocol study. Am J Hematol. 2023;98(4):598–607.

8. Vanhoenacker FM, Verlooy J, De Praeter M. Spontaneous resolution of unifocal Langerhans cell histiocytosis of the skull: potential role of ultrasound in detection and imaging follow-up. J Ultrason. 2018;18(74):265–70.
9. Chow TW, Leung WK, Cheng FWT, Kumta SM, Chu WCW, Lee V, et al. Late outcomes in children with Langerhans cell histiocytosis. Arch Dis Child. 2017;102(9):830–5.
10. Chen ED, Cheng P, Cai YF, Xiang YY, Zheng HM, Xing HX, et al. Ultrasonographic features of Langerhans cell histiocytosis of the thyroid. Int J Clin Exp Pathol. 2014;7(3):1229–35.
11. Morgan B, Lau HL, Yellin S. Cranium-Penetrating Mass Detected by Ultrasound Expedited Management of Langerhans Cell Histiocytosis. Pediatr Emerg Care. 2017;33(4):290–2.
12. Ji W, Ladner J, Rambie A, Boyer K. Multisystem Langerhans Cell Histiocytosis in an infant. Radiol Case Rep. 2021;16(7):1798–805.
13. Holley A. Sonographic diagnosis of unifocal Langerhans cell histiocytosis of the skull. J Clin Ultrasound. 2010;38(8):440–2.
14. DiPietro MA, Leschied JR. Pediatric musculoskeletal ultrasound. Pediatr Radiol. 2017;47(9):1144–54.
15. Kosiak W, Piskunowicz M, Swieton D, Bien E, Batko T. Sonographic diagnosis and monitoring of localized langerhans cell histiocytosis of the skull. J Clin Ultrasound. 2013;41(3):134–9.
16. Alston RD, Tatevossian RG, McNally RJ, Kelsey A, Birch JM, Eden TO. Incidence and survival of childhood Langerhans cell histiocytosis in Northwest England from 1954 to 1998. Pediatr Blood Cancer. 2007;48(5):555–60.
17. Kim BE, Koh KN, Suh JK, Im HJ, Song JS, Lee JW, et al. Clinical features and treatment outcomes of Langerhans cell histiocytosis: a nationwide survey from Korea histiocytosis working party. J Pediatr Hematol Oncol. 2014;36(2):125–33.
18. Concepcion W, Esquivel CO, Terry A, Nakazato P, Garcia-Kennedy R, Houssin D, et al. Liver transplantation in Langerhans' cell histiocytosis (histiocytosis X). Semin Oncol. 1991;18(1):24–8.
19. Morimoto A, Oh Y, Shioda Y, Kudo K, Imamura T. Recent advances in Langerhans cell histiocytosis. Pediatr Int. 2014;56(4):451–61.
20. Patten DK, Wani Z, Tolley N. Solitary langerhans histiocytosis of the thyroid gland: a case report and literature review. Head Neck Pathol. 2012;6(2):279–89.
21. Pandyaraj RA. Sathik Mohamed Masoodu K, Maniselvi S, Savitha S, Divya Devi H: Langerhans cell histiocytosis of thyroid-a diagnostic dilemma. Indian J Surg. 2015;77(Suppl 1):49–51.
22. Wake L, Xi L, Raffeld M, Jaffe ES. Langerhans cell histiocytosis, non-langerhans histiocytosis and concurrent papillary thyroid carcinoma with BRAF V600E mutations: a case report and literature review. Hum Pathol (N Y). 2019;17:200302.
23. David FA, Gabriel P, Kasumi M, Swee Hoe O, Albert H, Christian F, Philip HJ. Outcompeting p53-Mutant Cells in the Normal Esophagus by Redox Manipulation. Cell Stem Cell. 2019;25(3):329-341.e6.
24. Magda BdBG, Isabelle TC, Richard H, Michael H, Graham B, Maria-Odile B, Lucian LC, Jérémie D, Gilles F, Tore SI, et al. Risk of hematological malignancies from CT radiation exposure in children, adolescents and young adults. Nat Med. 2023;29(12):3111–9.
25. Maglie R, Vannucchi M, Quintarelli L, Caproni M, Massi D, Antiga E. At the Root: Cutaneous Langerhans Cell Histiocytosis. Am J Med. 2018;131(8):922–6.

Publisher's Note